Author Manuscript

Author Manuscript

Author Manuscript

Author Manuscript

HHS Public Access

Author manuscript

J Immunol. Author manuscript; available in PMC 2017 December 15.

Published in final edited form as:

J Immunol. 2016 December 15; 197(12): 4626–4638. doi:10.4049/jimmunol.1601488.

Overexpression of soluble Fas ligand following AAV gene therapy prevents retinal ganglion cell death in chronic and acute murine models of glaucoma

Anitha Krishnan[*], **Fei Fei**[*,†], **Alexander Jones**[*], **Patricia Busto**[§], **Ann Marshak-Rothstein**[§], **Bruce R. Ksander**[*,‡], and **Meredith Gregory-Ksander**[*,‡]

[*]Schepens Eye Research Institute, Massachusetts Eye and Ear Infirmary, Department of Ophthalmology, Harvard Medical School, Boston, MA, USA

[†]Department of Ophthalmology, Xijing Hospital, Fourth Military Medical University, Peoples Republic of China

[§]Department of Medicine, University of Massachusetts Medical School, Worcester, MA, USA

Abstract

Glaucoma is a multifactorial disease resulting in the death of retinal ganglion cells (RGCs) and irreversible blindness. Glaucoma-associated RGC cell death depends on the pro-apoptotic and proinflammatory activity of membrane-bound FasL (mFasL). In contrast to mFasL, the natural soluble FasL cleavage product (sFasL) inhibits mFasL-mediated apoptosis and inflammation and is therefore a mFasL antagonist. DBA/2J (D2) mice spontaneously develop glaucoma and predictably RGC destruction is exacerbated by expression of a mutated membrane-only FasL (mFasL) gene that lacks the extracellular cleavage site. Remarkably, one time intraocular adeno-associated virus-mediated gene delivery of sFasL (AAV2.sFasL) provides complete and sustained neuroprotection in both the chronic D2 and acute microbead-induced models of glaucoma, even in the presence of elevated intraocular pressure (IOP). This protection correlated with inhibition of glial activation, reduced production of TNFα, and decreased apoptosis of RGCs and loss of axons. These data indicate that cleavage of FasL under homeostatic conditions, and the ensuing release of sFasL, normally limits the neurodestructive activity of FasL. The data further support the notion that sFasL, and not mFasL, contributes to the immune privileged status of the eye.

Introduction

Glaucoma, a leading cause of blindness worldwide, is a complex multifactorial disease characterized by the progressive loss of retinal ganglion cells (RGCs) (1). While elevated intraocular pressure (IOP) is a well-recognized risk factor for the development of glaucoma, and remains the only modifiable disease-associated parameter, recent studies demonstrate that reduction of IOP alone does not prevent disease progression in all patients and that RGC destruction can continue even after IOP has been successfully lowered (2, 3). Moreover, the

Corresponding author: Meredith Gregory-Ksander, PhD, 20 Staniford Street, Boston, MA.02114, 617-912-7455, Meredith_gregory@meei.harvard.edu.

[‡]These authors contributed equally to this work

Author Manuscript Author Manuscript Author Manuscript Author Manuscript

high incidence of normal tension glaucoma (4, 5, 6) and the absence of neurodegeneration in some patients with elevated IOP (2, 7), indicates that IOP-***in****dependent* mechanisms also participate in the development and progression of glaucoma. As a result, current research is focused on developing neuroprotective therapies to complement conventional IOP lowering-drugs with the goal of preventing optic nerve degeneration and preserving vision.

Growing evidence in clinical and experimental studies over the past decade strongly suggest the involvement of the immune system in glaucoma (8, 9, 10). In experimental models of glaucoma, treatment with anti-inflammatory drugs such as minocycline (11) or treatment with antibodies that inhibit TNFα (12, 13) resulted in increased RGC survival. Enhanced RGC survival was also observed in mouse models of glaucoma where the infiltration of macrophages, present in both human and experimental models of glaucoma (13, 14, 15) was inhibited through the use of $Mac1^{-/-}$ mice (13) or ocular irradiation (15). Together these studies demonstrate a critical role for inflammation in the pathogenesis of glaucoma.

Fas Ligand (FasL) is a 40 kDa type II transmembrane protein of the TNF family, originally identified by its capacity to induce apoptosis in Fas receptor positive cells (16) and mediate activation induced cell death in T cells (17–19). However, there is increasing evidence that activation of the Fas receptor can also result in inflammation (20–23). FasL can be expressed as a membrane-bound protein (mFasL), that is both pro-apoptotic and proinflammatory, or cleaved and released as a soluble protein (sFasL) that inhibits both the apoptotic and inflammatory activity of mFasL (24–26). In vitro, we demonstrated that mFasL, but not sFasL, stimulated purified peritoneal macrophages and neutrophils to secrete the proinflammatory mediators MIP and IL1β (27, 28). As a result of its pro-apoptotic and proinflammatory functions, FasL is a potentially destructive molecule, whose expression is normally tightly regulated. One exception is in the eye where FasL is constitutively expressed in the cornea and retina (29). Importantly, in the context of experimental glaucoma, FasL expression is increased on resident microglial cells (27, 30) and the Fas/FasL signaling pathway is required for RGC death (27). However, in the eye, the form, as well as, the level of FasL expression is critical in determining the outcome of FasL expression (31, 32). We previously demonstrated that transduced ocular tumor cells expressing high levels of mFasL terminate immune privilege and induce a potent inflammatory response (31). By contrast, immune privilege was maintained and inflammation prevented in the presence of high levels of sFasL (31). Using a TNFα-induced “normal-tension” model of glaucoma we previously demonstrated that gene-targeted mice expressing only the membrane form of FasL exhibited accelerated RGC death and that a single intravitreal injection of recombinant sFasL provided short-term protection to RGCs in these mFasL-only mice (27). Together these data revealed a critical neurotoxic effector function for mFasL and neuroprotective function of sFasL in glaucoma.

In the current study, we further explored the neurodestructive function of mFasL and neuroprotective function of sFasL in the development and progression of glaucoma in two of the most widely used mouse models of elevated-IOP-induced glaucoma, the spontaneous genetic-based D2 (DBA/2J) mouse model and the microbead-induced mouse model. Our data reveal that mFasL participates in the development and progression of glaucoma through activating both apoptotic and non-apoptotic signaling pathways. In addition, AAV-mediated

Author Manuscript Author Manuscript Author Manuscript Author Manuscript

gene delivery of sFasL (AAV2.sFasL) to the retina provided long-term protection to RGCs and optic nerve axons in both the D2 chronic mouse model of glaucoma and the acute mouse model of microbead-induced elevated IOP. Together, these data reveal the pleotropic effects of sFasL on glial activation, inflammation, and apoptosis of RGCs and provide proof-of-principal that AAV2.sFasL can provide complete and sustained neuroprotection of RGCs in both chronic and acute mouse models of glaucoma, even in the presence of ongoing elevated IOP.

Materials and Methods

Animals

All animal experiments were approved by the Institutional Animal Care and Use Committee at Schepens Eye Research Institute and were performed under the guidelines of the Association of Research in Vision and Ophthalmology (Rockville, MD). The DBA/2J-Gpnmb $^{+}$/SjJ mice (D2-Gp) were purchased from Jackson Laboratories (Bar Harbor, ME). DBA/2J mice expressing only membrane FasL (this cleavage site deleted-mouse line was designated as D2-ΔCS) were produced by crossing the ΔCS founder mice (27) to DBA/2J mice purchased from Jackson Laboratories for 10 generations. After 10 generations, D2-ΔCS mice heterozygous for the ΔCS mutation were intercrossed to produce D2.ΔCS homozygous for the ΔCS mutation (D2-ΔCS) mice and WT littermates (D2). All three genotypes (D2, D2-ΔCS, and D2-Gp), were housed and maintained under cyclic light (12L-30 lux:12D) conditions in an AAALAC approved animal facility at the Schepens Eye Research Institute and equal number of males and females were used in each study. For the microbead studies, 8 week old C57BL/6J WT mice were purchased from Jackson laboratories (Bar Harbor, ME).

Viral Vector Construction

The Adeno-associated vectors, scAAV2-CB6-PI-eGFP and scAAV2-CB6-PI-sFasLecto, were prepared at the Gene Therapy Center (Dr. Gaungping Gao, University of Massachusetts Medical School, Worcester MA). The seed plasmid pAAVsc CB6 PI sFasLecto was made by isolating a 582 bp fragment corresponding to the full cDNA sequence of sFasL ecto 5”GCSF from pcDNA3-sFasL-ecto plus 5′ mGCSF (31). The 582 bp fragment was ligated (T4 ligase NEB #M0202) to a BamHI, HindIII double digested and Antartic phosphatase treated pAAVsc-CB6-PI plasmid provided by the Gene Therapy Center, UMMS. An aliquot of the ligation mixture was transfected onto E.Coli competent cells and plated onto LB-Agar plus 50 ug/ml Carbenicillin. Colonies were picked and grown on LB-Carbenicillin media, and plasmid mini-preps were checked by restriction enzyme and sequencing. A large scale of the plasmid was prepared from 1 liter of bacterial culture and isolated using a ZR Plasmid gigaprep kit (#D4056, Zymo Research, Irvine CA)

IOP measurements

IOP was measured with a rebound TonoLab tonometer (Colonial Medical Supply, Espoo, Finland), as previously described (27). Mice were anesthetized by 3% isoflurane in 100% oxygen (induction) followed by 1.5% isoflurane in 100% oxygen (maintenance) delivered with a precision vaporizer. IOP measurement was initiated within 2 to 3 min after animals

Author Manuscript Author Manuscript Author Manuscript Author Manuscript

lost toe pinch reflex or tail pinch response. Anesthetized mice were placed on a platform and the tip of the pressure sensor was placed approximately 1/8 inch from the central cornea. Average IOP was displayed automatically after 6 measurements after elimination of the highest and lowest values. This machine-generated mean was considered as one reading, and six readings were obtained for each eye. For D2.Gp, D2, and D2.ΔCS mice, IOPs were measured once a month. For the microbead study, baseline IOPs were obtained one day before microbead injection and the IOPs were then measured every three days after microbead injection. All IOPs were taken at the same time of day (between 10:00 and 12:00 hours) due to the variation of IOP throughout the day.

Intravitreal injections

The intravitreal injections, just posterior to the limbus-parallel conjunctival vessels, were performed as previously described (27). Mice received a 1μl intravitreal injection into both eyes containing AAV2.sFasL ($3x10^{12}$ PFU/ml) or AAV2.eGFP ($3x10^{12}$ PFU/ml) and sterile physiologic saline was used as a vehicle control.

Induction of elevated IOP

Mice were anesthetized by intraperitoneal injection of a mixture of ketamine (100 mg/kg; Ketaset; Fort Dodge Animal Health, Fort Dodge, IA) and xylazine (9 mg/kg; TranquiVed; Vedco, Inc., St. Joseph, MO) supplemented by topical application of proparacaine (0.5%; Bausch & Lomb, Tampa, FL). Elevation of IOP was induced unilaterally by injection of polystyrene microbeads (FluoSpheres; Invitrogen, Carlsbad, CA; 15-μm diameter) to the anterior chamber of the right eye of each animal under a surgical microscope, as previously reported (33, 34). Briefly, microbeads were prepared at a concentration of 5.0×10^6 beads/mL in sterile physiologic saline. The right cornea was gently punctured near the center using a sharp glass micropipette (World Precision Instruments Inc., Sarasota, FL). A small volume (2 μL) of microbeads was injected through this preformed hole into the anterior chamber followed by injection of an air bubble via the micropipette connected with a Hamilton syringe. Any mice that developed signs of inflammation (clouding of the cornea, edematous cornea etc) were excluded from the study.

Quantification of retinal ganglion cells

The neural retina was isolated and fixed in 4% paraformaldehyde for 2 hour at room temperature. Retinal flat mounts were incubated at 4 °C overnight with a primary antibody against an RGC-specific marker, β-III-tubulin (Millipore, Billerica, MA) (33, 34). An Alexa Fluor 594–conjugated secondary antibody (Invitrogen) was used as secondary antibody. Nuclei were counterstained with DAPI (Vector Stain). 60X oil-immersion was used and sixteen non-overlapping images were taken, with four-five images within each quadrant. All cells in ganglion cell layer positively labeled by the β-III-tubulin antibody were counted. Retinal areas were measured using Image J software, and the RGC density/mm^2 retina was calculated.

Author Manuscript Author Manuscript Author Manuscript Author Manuscript

Quantification of optic nerve axons

For quantification of axons, optic nerves were dissected and fixed in karnovsky's reagent (50% in phosphate buffer) overnight. Semi-thin cross-sections of the nerve were taken at 1.0 mm posterior to the globe and stained with 1% p-phenylenediamine (PPD) for evaluation by light microscopy. Ten non-overlapping photomicrographs were taken at 100× magnification covering the entire area of the optic nerve cross-section. The total area of each optic nerve cross-section was determined with Image J software and this value was used to estimate the total axon density per optic nerve cross-section.

TUNEL staining

Apoptotic cells were evaluated by TUNEL staining. Eyes were enucleated, fixed in 10% formalin. Eyes were processed and 20 μm paraffin sections mounted on slides were used for staining. The sections were de-paraffinized before staining for TUNEL according to the manufacturer's protocol (In Situ Cell Death Detection Kit; Roche Applied Science, Mannheim Germany, 11684795910) as previously described (25). The sections were mounted using VECTARSHIELD Mounting Medium with DAPI (Vector Laboratories, H-1200). Sections were washed, cover slipped and examined by confocal laser scanning microscopy ((Leica Microsystems and processed using SP6 software).

Quantitative RT-PCR

At the time point for euthanasia anesthetized mice were perfused through the left ventricle with 10 ml of 1xPBS. Following perfusion, the eyes were enucleated and RNA was isolated from the neural retina using Qiagen RNeasy mini kit (Cat # 74104) according to the manufacturer's protocol. RNA was treated with DNAse (Cat # AM222, Invitrogen) to ensure no contamination of genomic DNA. 500ng of RNA was used to prepare cDNA using the iScript cDNA synthesis kit from Bio-Rad (Cat # 170-8890) according to the manufacturer's protocol. cDNA was treated with RNaseH (18021-014, Invitrogen) to ensure absence of single stranded RNA. Quantitative real time PCR was performed using the master mix from Invitrogen (Cat # 4472903) using the manufacturer's protocol in 10μl total volume in duplicates. Relative expression to house keeping gene β-actin was quantified using the formula: Relative expression =10,000 x 1/2^(Avg. Gene cT- Avg. β-actin cT). All of the primers used are listed in Table I.

Western blot analysis

To assess total FasL expression in the posterior segments of D2, D2-Gp, and D2-ΔCS mice, protein lysates (20μg/sample) were prepared from posterior eye cups (neural retina, choroid, and sclera) as previously described (27). To assess over expression of sFasL in the neural retina of AAV2 treated eyes, protein lysates (5ug/sample) were prepared from the neural retina only. Proteins were separated on 12% Tris-glycine gels (Invitrogen, Carlsbad CA) and transferred to polyvinylidene difluoride membranes (Invitrogen, Carlsbad CA). The membranes were probed for Fas ligand using a polyclonal rabbit anti-Fas ligand antibody (25) followed by an IRDye secondary antibody (Li-Cor Biotechnology, Lincoln NE). Mouse β actin was used to assess equal loading. Each blot was developed using the LI-COR Odyssey imaging system (LI-COR Biotechnology, Lincoln NE). Densitometry was

Author Manuscript Author Manuscript Author Manuscript Author Manuscript

performed using Image Studio software. L5178Y-R tumor transfectants over expressing sFasL or mFasL (25, 27) were used as positive controls and a protein lysate prepared from a posterior eyecup prepared from FasL-KO mice (28, 35) was used as a negative control.

Statistics

"All data are presented as mean ± SEM and Graph Pad Prism 6 (La Jolla, CA, USA) was used to perform statistical analysis of the data For comparisons in the D2.ΔCS studies, one-way ANOVA and Tukeys multiple comparison test were used. For comparisons in the D2-AAV2 studies, two-way ANOVA and Tukey's multiple-comparison test were used. For comparisons in the microbead-model studies, two-way ANOVA and Sidak's multiple-comparison test were used. A P-value of less than 0.05 was considered significant.

Results

Accelerated glaucoma in D2.ΔCS mice

DBA/2J (D2) mice spontaneously develop age-related elevated intraocular pressure (IOP) due to mutations in Gpnmb and Tyrp1 genes that trigger iris stromal atrophy and pigment dispersion, respectively (36, 37). As a result, D2 mice develop elevated IOP by approximately 6–8 months of age, followed by the loss of RGCs and nerve fibers. We previously demonstrated that D2 mice expressing only mFasL (D2-ΔCS) displayed marked thinning of the nerve fiber layer at 5 months of age that was not seen in D2 mice that expressed WT FasL (27). Early thinning of the nerve fiber layer suggested that the development of glaucoma was accelerated. However, our previous study did not include a quantitative analysis of RGCs, optic nerve axons or apoptosis in the neural retina. To confirm the accelerated development of glaucoma in D2-ΔCS mice, we performed quantitative analysis of RGCs and axons and correlated this data with accelerated apoptosis in the neural retina. In addition, we now have age- and strain-matched control D2-Gp ($DBA/2J^{Gpnmb+/+}$) mice that do not develop glaucoma. These control D2-Gp congenic mice express a normal Gpnmb gene and develop a very mild form of iris disease due to the Tyrp1 mutation, but do not develop elevated IOP or glaucoma. To perform our analysis, we compared disease progression in young and old D2-ΔCS mice with D2 littermates that express WT FasL (positive control) and the D2-Gp mice that do not develop elevated IOP or glaucoma (negative control) (38). IOP was measured using rebound tonometry at 3, 6 and 9 months of age (Figure 1A). D2 and D2-ΔCS mice displayed elevated IOP beginning at 6 months of age, as compared with the negative control D2-Gp mice. However, there were no significant differences in IOP between D2 and D2-ΔCS mice at any age, indicating the ΔCS mutation does not affect IOP.

To determine whether the loss of RGCs and/or axons was accelerated in D2-ΔCS mice, groups of mice were euthanized at 3 and 6 months of age and retinal flat mounts were stained with the RGC-specific marker βIII tubulin to assess RGC density and optic nerve sections were stained with paraphenylenediamine (PPD) to assess axon density. As reported previously, the loss of RGCs and axons in D2 mice is age-related and only develops in mice >8 months old (36, 37, 39). Therefore, at 3 and 6 months of age D2 displayed no significant loss of RGCs or axons, as compared with D2-Gp mice (Figure 1B, C, D, E). By contrast,

Author Manuscript Author Manuscript Author Manuscript Author Manuscript

D2-ΔCS mice developed early loss of RGCs and axons at 6 months, indicating expression of non-cleavable FasL in D2-ΔCS mice results in accelerated development of glaucoma.

Numerous studies demonstrate that RGCs die by apoptosis during glaucoma (40–42). To demonstrate the accelerated death of RGCs in D2-ΔCS mice was due to apoptosis, TUNEL staining was performed on retinal sections from D2, D2-ΔCS, and D2-Gp mice at 3 months (Figure 2A, B) and 6 months (Figure 2C, D) of age. TUNEL+ cells were detected in the RGC layer of D2-ΔCS at both 3 and 6 months of age, as compared with D2 and D2-Gp mice. Moreover, at 6 months of age, the TUNEL positive cells detected in D2-ΔCS mice were no longer restricted to the RGC layer (Figure 2C). Together, these results indicate that D2-ΔCS mice display early death of RGCs via apoptosis, resulting in accelerated development of glaucoma.

Expression of Fas, FasL and FADD in D2-ΔCS mice

While previous studies demonstrated FasL was upregulated in the retina following elevated IOP (25, 26) the levels of sFasL and mFasL were not assessed. To determine the effects of elevated IOP on components of the Fas-induced apoptosis pathway in D2 and D2-ΔCS mice, the neural retina was analyzed by quantitative RT-PCR for the mRNA levels of Fas, FasL, and the Fas activating death domain (FADD) and Western blots were performed to quantitate protein expression. The Western blot for FasL was prepared from lysates of the posterior segment of the eye (retina, choroid, and sclera) which detected the smaller 26 kD sFasL band, as well as, two larger 34 kD and 38 kD mFasL bands (Figure 3D). The two mFasL bands (34 and 38 kD) were reported previously and represent differential glycosylation of mFasL (25, 27, 43, 44). The two forms of FasL (mFasL and sFasL) were present in the posterior segment from all three groups of mice (D2-Gp, D2, and D2-ΔCS mice). As an important specificity control for the Western blot, posterior eye segment lysates from FasL KO mice confirmed the loss of sFasL (26 kD band) and mFasL (34 and 38 kD bands). As expected, no sFasL was detected in the eye tissue from D2-ΔCS mice (Figure 3D), proving the knock-in mutation of the FasL cleavage site prevents expression of sFasL in the retina.

There was no significant difference in Fas expression (mRNA and protein levels) between D2-Gp, D2, and D2-ΔCS mice at 3 or 6 months of age (Figure 3A and 3E). While there was a trend toward reduced Fas mRNA expression in the D2-ΔCS mice at 6 months, the difference was not statistically significant (P=0.15, Figure 3A). These data indicate that Fas expression in all three groups of mice remained constant and therefore cannot account for the accelerated development of glaucoma at 6 months in D2-ΔCS mice.

In contrast with the constant Fas levels, there was a significant age-related increase in mFasL and FADD mRNA between 3–6 months in D2-ΔCS mice, which coincided with the beginning of RGC death at 6 months of age. Moreover, in D2 and D2-Gp mice, which displayed no RGC loss at 6 months, the levels of mFasL and FADD (mRNA and protein levels) were significantly reduced as compared with D2-ΔCS mice (Figure 3B, D and 3C, F). Previous work by our laboratory (27) and Ju et al., (30) demonstrated that within the neural retina, FasL is primarily expressed on microglia in the ganglion cell layer and inner nuclear layer of non-glaucomatous eyes. In glaucomatous eyes, FasL is expressed on microglia (and/or infiltrating macrophages) at higher levels and coincided with apoptosis of RGCs (27,

Author Manuscript Author Manuscript Author Manuscript Author Manuscript

30). Thus the increased FasL expression in glaucomatous D2-ΔCS mice may account for the trend toward reduced Fas expression (Figure 3A) as some Fas+ cells are induced to undergo apoptosis. Increased engagement of the remaining Fas may also account for the increase in FADD. Together, these data indicate the accelerated disease development in D2-ΔCS mice coincided with an increase in the expression of the neurotoxic mFasL and FADD, the adapter protein required for the formation of the death-inducing signaling complex during apoptosis.

Importantly, our Western blot analysis of mFasL and sFasL in the posterior segment of the eye showed that sFasL was the predominant form of FasL expressed in the retina of mice that possess the WT allele for FasL (D2-Gp and D2 mice). Therefore, in non-diseased retinas, under homeostatic conditions, most FasL is cleaved to release neuroprotective sFasL. It follows that the development of glaucoma in D2 mice coincides with a shift from the production of neuroprotective sFasL to neurodestructive mFasL.

Muller cell activation in D2-ΔCS mice

Muller cells, which span all retinal layers, constitute the principal glial cells of the retina and provide support to retinal neurons (45). In the normal retina, glial fibrillary acidic protein (GFAP) is expressed in the nerve fiber layer by astrocytes and also in the end feet of Muller cells (29, 39). However, in glaucoma, GFAP expression is markedly increased in Muller cells as a result of reactive gliosis, which is considered a key indicator of neuroinflammation (30, 46, 47). To monitor Muller cell activation, GFAP mRNA expression in the retina was quantified by RT-PCR, and protein levels were assessed by immunohistochemical staining using an anti-GFAP antibody. D2, D2-ΔCS, and D2-Gp mice were examined at 3 and 6 months of age. At 3 months of age, GFAP expression was restricted to astrocytes and Muller cell-end-feet in the nerve fiber layer in all three groups of mice and there was no significant difference in expression of GFAP mRNA among the 3 strains of mice (Figure 4A, B). However, by 6 months of age, expression of GFAP in D2-ΔCS mice was no longer limited to astrocytes and Muller cell-end-feet in the nerve fiber layer, but extended throughout the whole length of retinal Muller cells. This correlated with a modest but significant increase in GFAP mRNA levels in the D2-ΔCS mice, as compared to the D2 and D2-Gp groups (Figure 4 A, B). The increase in GFAP coincided with a significant increase in TNFα mRNA levels in D2-ΔCS mice as compared to D2 and D2-Gp mice (Figure 4C). TNFα is an immediate early gene that is rapidly transcribed in response to signals of stress and inflammation and is often used as a measure of macrophage and glial activation (48–52). In regards to glaucoma, a variety of rodent animal models have implicated glial-cell produced TNFα in the pathogenesis of elevated IOP-induced glaucoma (12, 13, 53, 54). These models include: rat episcleral vein cauterization model (13), mouse laser-induced photocoagulation of the limbus model (12), and the spontaneous D2 model (53, 54). These data indicate that accelerated loss of RGCs in D2-ΔCS mice that express high levels of mFasL coincides, not only with the induction of apoptosis of RGCs, but also with glial activation and the induction of the immediate early gene, TNFα.

Author Manuscript Author Manuscript Author Manuscript Author Manuscript

Intravitreal delivery of sFasL using AAV2

The membrane-bound form of FasL is responsible for both the induction of apoptosis and for proinflammatory cytokine production and therefore the exacerbated development of glaucoma in the D2-ΔCS mice can be explained by the increased expression of uncleaved mFasL. However, sFasL has been shown to serve as an mFasL antagonist that blocks FasL-induced apoptosis and inflammation (25, 26). Moreover, we previously found that a single intravitreal injection of recombinant sFasL protein can protect the nerve fiber layer in the short-term model of TNFα-induced glaucoma (27). Therefore, it was important to determine whether sFasL could also block the effects of mFasL in the widely accepted mouse models of spontaneous and induced elevated IOP glaucoma models.

Previous studies demonstrated that an intravitreal injection of AAV2 vectors in mice results primarily in transduction of long-lived RGCs and cells of the inner nuclear layer (57–59). As a result, gene delivery using AAV2 can provide long-term consistent expression within the inner retina. To evaluate which retinal cells were transduced, an AAV2 vector expressing only eGFP (AAV.eGFP) was injected into the vitreous of two month-old D2 mice. Confocal microscopy was used to assess eGFP expression in retinal whole mounts at 2 weeks post injection and showed uniform eGFP distribution throughout the retina (Figure 5A). Cross sectional reconstruction of the retina showed strong eGFP expression throughout the ganglion cell layer and inner nuclear layers (Figure 5B).

To determine whether we could maintain long-term sFasL expression in the retina of D2 mice, we used AAV2 vectors to deliver a gene encoding sFasL to the RGCs of D2 mice via a single intravitreal injection. Western blot analysis of cells isolated from the neural retina showed a significant increase in sFasL expression as early as 2 weeks post injection, as compared to D2 mice treated with either AAV2.eGFP or uninjected control mice (Figure 5C). Moreover, the increase in sFasL in the retina was sustained at a consistent level throughout the length of the study (8 months) following a single injection. Monthly monitoring of IOP revealed no significant differences in IOP levels at any age between D2 uninjected control mice and D2 mice that received either AAV2.eGFP or AAV2.sFasL treatment (Figure 5D). Furthermore, representative slit lamp images taken at 9 months of age showed no differences in the severity of either iris pigment dispersion or iris atrophy between D2 uninjected control mice and D2 mice that received either AAV2.eGFP or AAV2.sFasL treatment (Figure 5D). Taken together, these results demonstrate that a single intravitreal injection of AAV2.sFasL into D2 mice produces long-term stable expression of high levels of sFasL within the inner retina, which has no effect on the development of: iris pigment dispersion, iris atrophy, and elevated IOP.

Intravitreal delivery of AAV2.sFasL prevents loss of RGCs and axons and provides long-term protection in D2 mice

To determine whether over expression of sFasL prevents the loss of RGCs and axons in D2 mice, mice received an intravitreal injection of AAV2.sFasL at 2 months of age and were euthanized 8 months later at 10 months of age. RGC density was measured in retinal whole mounts stained with anti-βIII tubulin antibody and axon density was measured in optic nerve sections. As expected in D2-uninjected mice and D2-AAV2.eGFP mice at 10 months of age,

Author Manuscript Author Manuscript Author Manuscript Author Manuscript

there was a significant decrease in both RGC and axon density as compared to the D2-Gp negative control mice that do not develop glaucoma (Figure 6A–D). By contrast, D2 mice treated with AAV2.sFasL displayed no significant loss in either RGC or axon density as compared with D2-Gp control mice (Figure 6B, D). To demonstrate that AAV2.sFasL treatment provides long-term protection and does not just delay the death of RGCs and axons, additional groups of mice were followed for up to 15 months of age. Quantification of RGCs and axons revealed that even at 15 months of age, the AAV2.sFasL treated D2 mice continued to display significant protection of RGCs and axons when compared with D2-uninjected mice and AAV2.eGFP mice (Figure 6E–H). In conclusion, these data demonstrate that overexpression of sFasL resulting from a single intravitreal injection provides complete and long-term protection to the RGCs and axons in D2 mice, even in the presence of elevated IOP.

sFasL prevents activation of pro-inflammatory Muller cells in D2 mice

As we previously demonstrated (Figure 4A, B, C), loss of RGCs in glaucomatous D2 mice coincided with activation of Muller cells that express GFAP and the induction of TNFα. To determine whether the absence of glaucoma in AAV2.sFasL treated D2 mice coincided with reduced Muller cell activation, GFAP expression in Muller cells was determined by immunohistochemical staining and RT-PCR was used to measure GFAP and TNFα mRNA expression in the neural retina of 10 month old: D2-untreated, D2-AAV2.eGFP, D2-AAV2.sFasL, and D2-Gp mice. As expected, D2-untreated and D2-AAV2.eGFP mice that develop glaucoma displayed activated pro-inflammatory Muller cells that express high levels of GFAP as seen in confocal images (Figure 7A) and RT-PCR revealed a significant increase in GFAP and TNFα mRNA expression (Figure 7B, C). By contrast, in D2-AAV2.sFasL mice that do not develop glaucoma, Muller cells express significantly less GFAP and TNFα mRNA levels were equivalent to those seen in D2-Gp normal control mice (Figure 7A, B, C). These data demonstrate that in D2-AAV2.sFasL mice the sFasL-mediated protection of RGCs and axons coincides with preventing activation of Muller cells and induction of the immediate early gene, TNFα.

sFasL prevents upregulation of apoptotic genes and downregulation of pro-survival genes in D2 mice

In glaucoma, both extrinsic and intrinsic pathways of apoptosis have been identified as mediators of RGC apoptosis (12, 27, 60–62). To determine whether treatment with sFasL inhibited the induction of both extrinsic and intrinsic pathways of apoptosis, qRT-PCR was performed on retinal tissue from D2, D2-Gp, D2-AAV2.eGFP, and D2-AAV2.sFasL mice at 10 months of age to assess the expression of apoptotic genes and pro-survival genes. At 10 months of age, there were two distinct gene expression patterns in untreated D2 mice as compared with sFasL treated D2 mice. In untreated D2 mice, pro-apoptotic genes in both intrinsic (BAX) and extrinsic (Fas, FADD) pathways of apoptosis were upregulated, while anti-apoptotic genes (cFLIP, Bcl2, cIAP-2) were down regulated. By contrast, mice treated with sFasL prevented both the induction of pro-apoptotic genes and downregulation of anti-apoptotic genes (Figure 7D and E). In D2 and D2-AAV.eGFP mice, the expression of pro-apoptotic genes Fas, FADD, and BAX were elevated in comparison to D2-Gp controls (Figure 7D). However, D2 mice treated with AAV2.sFasL prevented the upregulation of

Author Manuscript Author Manuscript Author Manuscript Author Manuscript

these genes (Fas, FADD, and BAX), which were equal to the levels detected in the D2-Gp control mice (Figure 7D). Similarly, the levels of the pro-survival genes (cFLIP, Bcl2, and cIAP-2) (Figure 7E) were down regulated in D2 and D2-AAV2.eGFP mice, but D2 mice treated with AAV2.sFasL prevented the downregulation of these genes, which were equal to the levels detected in the D2-Gp control mice. While mRNA expression does not always predict protein expression, these data indicate that (i) genes in both the intrinsic and extrinsic pathways of apoptosis are induced in glaucomatous D2 mice, which is in agreement with previous studies (53, 54, 61, 62), and (ii) treatment with sFasL prevents the induction of both of these pathways. Together, these results suggest that sFasL acts as an antagonist and prevents the binding of mFasL to the Fas receptor. Therefore, sFasL is preventing the mFasL-induced up-regulation of pro-apoptotic genes and the mFasL-induced down regulation of anti-apoptotic genes.

sFasL prevents loss of RGCs and axons in a microbead-induced model of glaucoma

To demonstrate that the neuroprotective effect of sFasL was not limited to the D2 model of glaucoma, we tested whether sFasL prevented RGC loss in a microbead-induced mouse model of elevated IOP, where an injection of microbeads into the anterior chamber of the eye obstructs the aqueous humor outflow and induces elevated IOP (33, 34). C57BL/6 mice received an intravitreal injection of AAV2.eGFP or AAV2.sFasL followed three weeks later by an anterior chamber injection of microbeads or saline as a negative control. At four weeks post microbead or saline injection, Western blot analysis confirmed the overexpression of sFasL in the neural retina of AAV2.sFasL treated mice as compared to the AAV2.eGFP treated mice (Figure 8A). As previously demonstrated (33,34) a single anterior chamber injection of 15μm polystyrene microbeads resulted in elevated IOP for up to 21 days in both AAV2.eGFP and AAV2.sFasL mice as compared to saline controls (Figure 8B). IOPs peaked at 11 days post microbead injection and there was no significant difference in the time course or magnitude of the microbead-induced elevated IOP between AAV2.sFasL or AAV2.eGFP treated mice, indicating sFasL did not affect IOP. Quantification of RGC density at 4 weeks post microbead injection revealed a significant decrease in RGC density in microbead-injected AAV2.eGFP treated mice as compared to the saline-injected control (Figure 8C, D). However, treatment with AAV2.sFasL protected RGCs and the RGC density in microbead-injected AAV2.sFasL mice was equal to the RGC density in the saline-injected controls (Figure 8C, D). Similar results were observed in the optic nerve where AAV2.sFasL treatment afforded complete protection of axons as compared to the AAV2.eGFP treated control group (Figure 8E, F). Taken together, these results demonstrate that AAV2.sFasL provides complete neuroprotection in both the chronic D2 and the acute microbead-induced models of elevated IOP.

Discussion

FasL is constitutively expressed in a variety of cells in the eye and other immune privileged sites where it has been implicated in the deletion of activated Fas-expressing effector cells and therefore the prevention of inflammation (29, 64). However, this protective activity of FasL has been challenged by numerous examples of FasL-associated ocular and CNS pathologies (22, 27, 30, 65, 66). For example, FasL has been shown to play a major role in

Author Manuscript Author Manuscript Author Manuscript Author Manuscript

animal models of glaucoma where it contributes to the death of Fas+ RGCs (27, 30). This apparent dichotomy, constitutive expression of FasL in non-diseased eyes and the association of FasL with numerous ocular pathologies, can be explained by the isoform of expressed FasL. Membrane-bound FasL is clearly proapoptotic and proinflammatory, but can be cleaved to release a soluble molecule that is incapable of mediating either cell death or apoptosis and in fact has been found to antagonize the activity of mFasL (24–26). However, the actual role of membrane vs soluble FasL at immune privileged sites has not been carefully examined.

Herein, we show that under homeostatic conditions, FasL in the eye is primarily cleaved to the soluble form and is therefore anti-inflammatory. Exactly how the balance between sFasL and mFasL shifts during diseases such as glaucoma is unclear, but our data demonstrate that mFasL is definitely the pathogenic isoform. We have explored the role of mFasL vs sFasL in gene-targeted ΔCS mice where the FasL cleavage site has been mutated and can no longer be cleaved by metalloproteinases (27, 67). In ΔCS mice, total FasL expression is controlled by the endogenous FasL promoter as in WT mice, but in ΔCS mice, cells that normally express FasL can only make mFasL and not sFasL. As a result, ΔCS mice develop accelerated and exacerbated destruction of retinal cells in both spontaneous and inducible models of glaucoma (27; current study). These data point to a key role for mFasL in glaucoma pathogenesis. The current study now demonstrates that sFasL can prevent the development of glaucoma.

We previously demonstrated that a single intravitreal administration of recombinant sFasL protein provided short-term protection to RGCs in a TNFα-induced “normal-tension” model of glaucoma (28). However, clinically glaucoma is a slow progressing chronic disease, requiring a treatment that can provide long-term protection. To further explore the function of sFasL in glaucoma, we constructed AAV-vectors that incorporated the genes for GFP or sFasL and injected them into the vitreous cavity of WT mice. GFP expression was monitored *in vivo* by fundus examination and confirmed *in vitro* by confocal microscopy of retinal flat mounts. We found that GFP was expressed in the RGC layer and inner nuclear layer for at least 8 months following a single injection. Likewise, Western blots confirmed sFasL expression in the neural retina of AAV-sFasL mice extended over the same time period. Importantly AAV-sFasL gene therapy resulted in complete long-term neuroprotection of RGCs and axons of the optic nerve, even in the continued presence of elevated IOP, in both spontaneous and inducible models of glaucoma. Therefore the increased disease severity in ΔCS mice most likely reflects excessive mFasL expression, as well as, the absence of sFasL-dependent inhibition.

Fas ligand is a 40-kDa Type II transmembrane protein that was initially identified as an inducer of apoptosis in Fas expressing cells (16). Using a TNFα-induced “normal-tension” model of glaucoma we previously demonstrated that gene-targeted mice expressing only mFasL exhibited accelerated RGC death. However, in addition to the proapoptotic effects of mFasL, the results of our current study indicate that mFasL also plays a role earlier in the pathogenesis of glaucoma via non-apoptotic pathways. FasL is known to directly and rapidly promote the transcription and secretion of a number of proinflammatory cytokines and neutrophil chemokines (28, 31, 68) that likely account for the massive neutrophil influx

Author Manuscript Author Manuscript Author Manuscript Author Manuscript

following the injection of FasL-transfected cells and tumors (31). FasL can also induce the processing of IL-1β and IL-18 through an inflammasome independent caspase 8-dependent mechanism (68). GFAP is a well-known marker of glial activation and is significantly increased in retinal astrocytes and muller cells following elevated IOP (46, 47, 69). As indicated by RT-PCR and immunofluorescence, we have now shown a significant increase in the expression of GFAP that occurs much earlier in D2-ΔCS mice than D2-WT mice. This early upregulation of GFAP indicates accelerated activation of glial cells in D2-ΔCS mice. Moreover, the accelerated glial activation in D2-ΔCS mice also correlated with an earlier induction of TNFα when compared to D2-WT mice. There is substantial evidence that TNFα is induced following elevated IOP (10, 12, 13, 53, 54,70) and is required for the death of RGCs (12, 13). Using the TNFα-induced model of glaucoma (12), we previously demonstrated that TNFα increased the expression of mFasL on retinal microglia and/or infiltrating macrophages and that Fas-FasL signaling was required for TNFα-mediated death of RGCs (28). While retinal microglia are also a cellular source for TNFα following elevated IOP (12, 13), in the absence of Fas or FasL, RGCs are protected from apoptosis (27). Taken together with the current study, these data suggest that TNFα and mFasL may form a positive feed-forward-loop where TNFα upregulates mFasL expressed on retinal microglia and mFasL induces apoptosis of RGCs while at the same time feeding back on the microglia and/or infiltrating macrophages to upregulate TNFα, thus leading to chronic neuroinflammation. The ability of AAV2.sFasL to prevent induction of TNFα, as well as, the apoptosis of RGCs suggest that sFasL directly blocks FasL-induced apoptosis of RGCs, while at the same time inhibits the TNFα-FasL positive feed-forward- loop, effectively shutting down neuroinflammation.

The eye has long been considered an immune privileged site as evidenced by the high acceptance rate of HLA unmatched allogeneic corneal transplants in uncomplicated or “low-risk” patients in which the recipient graft bed shows no sign of inflammation and/or neovascularization (71, 72). However, corneal immune privilege is not universal as demonstrated by the high rejection rate of allogeneic corneal transplants in “high-risk” patients in which donor tissue is transplanted into a recipient with on-going corneal inflammation and/or neovascularization (73). FasL was first implicated in maintaining immune privilege when it was shown that FasL-deficient corneal allografts were readily rejected (29, 74). However, overexpression of mFasL on the donor cornea, as a result of viral transfection, resulted in accelerated transplant rejection associated with innate-mediated inflammation (75). Together these data suggest that the soluble isoform may be responsible for the acceptance of corneal allografts in low-risk patients and raise the possible application of sFasL gene therapy for facilitating acceptance of corneal allografts in high-risk patients.

Over the past decade gene therapy has been tested in animal models of glaucoma as a treatment for glaucoma, delivering: neurotrophins (58), anti-apoptotic genes (57), and transcription factors (76) to the retina. There is substantial evidence in both human and experimental glaucoma animal models that RGCs die by apoptosis, but the molecular mechanisms that trigger apoptosis are not well understood (40–42). However, it is clear that simply blocking the apoptotic pathway in RGCs does not prevent completely neurodegeneration in glaucoma. This was illustrated in studies by Libby et al., who demonstrated that RGC somata of Bax-deficient D2 mice survived indefinitely in the

Author Manuscript Author Manuscript Author Manuscript Author Manuscript

presence of elevated IOP, while the axons continued to degenerate distal to the optic nerve head (61). In a related study by McKinnon et al., treatment with an adeno-associated virus (AAV) vector expressing baculoviral IAP repeat-containing protein-4 (BIRC4), a potent inhibitor of Caspase-3, -7, and -9, was only able to protect 50% of optic nerve axons (77), demonstrating that blocking only the apoptotic pathway in the RGCs is not sufficient to prevent glaucoma completely.

Several hypotheses have been proposed regarding the mechanism(s) that induce axonal degeneration and death of RGCs including oxidative stress (78), ischemia (79), excitotoxicity (80), and mitochondrial dysfunction (8). Although targeting these pathways has been successful in experimental models of glaucoma, these strategies have generally failed to translate into clinical success. This failure may be due to multiple reasons, including the lack of a suitable animal model, as well as, the fact that glaucoma is a multifactorial disease where numerous factors interact during disease progression. Therefore, the most effective neuroprotective strategy should target more than one pathway, work long-term, and show efficacy in more than one animal model of glaucoma.

AAV viral vectors have proven to be very effective at delivering transgenes to the retina and providing long-term gene expression that persists in the adult retina for over a year (81, 82). In particular, the AAV2 serotype specifically targets the cells of the ganglion cell layer and inner nuclear layer following an intravitreal injection (81). A recent report by Sullivan et al., demonstrated that AAV-mediated delivery of erythropoietin (AAV.EPOR76E) protected RGCs and axons in the D2 model of glaucoma (83). However, an additional study was performed to determine if the AAV.EPOR76E could also protect RGC axons in the mouse microbead occlusion model of elevated IOP and while the AAV.EPOR76E treated group appeared to have fewer degenerating axons when compared to the untreated group, there was no significant difference in the total number of axons between groups (84).

In the current study using AAV2.sFasL, we provide the first direct evidence of a virus-mediated gene therapy that provides complete and long-term protection, out to 15 months of age, of both RGCs and axons of the optic nerve in the chronic D2 mouse model of glaucoma. Treatment with AAV2.sFasL inhibited multiple pathways activated in the pathogenesis of glaucoma in the D2 mice including activation of retinal glial cells, induction of TNFα, and death of RGCs and axons, even in the presence of elevated IOP. Moreover, the efficacy of this gene therapy was even further validated in a second mouse microbead occlusion model of elevated IOP, again revealing complete protection of RGCs and axons. Exactly how sFasL attenuates mFasL activity remains to be determined. The sFasL may simply bind to Fas but fail to effectively crosslink the receptor, while at the same time preventing activation of the receptor complex by the membrane-bound form. Alternatively, sFasL may actively engage the receptor and lead to its internalization. Further studies will also need to address how the appropriate balance between sFasL an mFasL is maintained under normal conditions, and then disrupted under pathological conditions.

Acknowledgments

Grant support: The study was supported by the NIH Core grant P30EY003790 (Schepens) and NIH grants AR055634 (AMR) and EY021543 (MGK).

Author Manuscript Author Manuscript Author Manuscript Author Manuscript

The authors would like to thank Philip Seifert from morphology core at Schepens Eye Research Institute for processing and PPD staining of optic nerves. We would also like to thank Dr. Guangping Gao and the Gene Therapy center and Vector Core at the University of Massachusetts Medical School for producing the AAV2.sFasL and AAV2.eGFP vectors.

Non-standard abbreviations

RGC	retinal ganglion cell
IOP	intraocular pressure
FasL	Fas ligand
sFasL	soluble Fas ligand
mFasL	membrane-bound Fas ligand
AAV	adeno-associated virus
PPD	p-phenylenediamine
GFAP	Glial fibrillary acidic protein
cFLIP	cellular FADD-like IL-1β-converting enzyme-inhibitory protein
FADD	Fas-associated death domain
BAX	bcl-2-like protein 4
Bcl2	B-cell lymphoma 2
cIAP-2	cellular inhibitor of apoptosis protein-2

References

1. Casson RJ, Chidlow G, Wood JP, Crowston JG, Goldberg I. Definition of glaucoma; clinical and experimental concepts. Clin Exp Ophthalmol. 2012; 40(4):341–349. [PubMed: 22356435]
2. Kass MA, Heuer DK, Higginbotham EJ, Johnson CA, Keltner JL, Miller JP, Parrish RK, Wilson MR, Gordon MO. The Ocular Hypertension Treatment Study. Arch Ophthalmol. 2002; 120:701–713. [PubMed: 12049574]
3. Heijl A, Leske C, Bengtsson B, Hyman L, Bengtsson B, Hussein M. Reduction of intraocular pressure and glaucoma progression. Arch Ophthalmol. 2002; 120:1268–1279. [PubMed: 12365904]
4. Mudumbai RC. Clinical update on normal tension glaucoma. Sem Ophthalmol. 2013; 28(3):173–179.
5. Sommer A, Tielsch JM, Katz J, Quigley HA, Gottsch JD, Javitt J, Singh K. Relationship between intraocular pressure and primary open angle glaucoma among white and black aemricans-The Baltimore Eye Survey. Arch Ophthalmol. 1999; 109:1090–1095.
6. Song BJ, Caprioli J. New directions in the treatment of normal tension glaucoma. Indian J Ophthalmol. 2014; 62(5):529–537. [PubMed: 24881596]
7. Leibowitz HM, Krueger DE, Maunder LR, Milton RC, Kini MM, Kahn HA, Nickerson RJ, pool J, Colton TL, Ganley JP, Loewenstein JI, Dawber TR. The Framingham Eye Study monograph: an ophthalmological and epidemiological study of cataract, glaucoma, diabetic retinopathy, macular degeneration, and visual acuity in a general population of 2631 adults, 1973–1975. Surv Ophthalmol. 1980; 24(suppl):335–610. [PubMed: 7444756]
8. Tezel G. The Role of Glia, Mitochondria, and the Immune System in Glaucoma. Invest Ophthalmol Vis Sci. 2009; 50:1001–1012. [PubMed: 19244206]

Author Manuscript Author Manuscript Author Manuscript Author Manuscript

9. Rieck J. The Pathogenesis of Glaucoma in the Interplay with the Immune System. Invest Ophthalmol Vis Sci. 2013; 54:2393–2409. [PubMed: 23539162]
10. Yang X, Luo C, Cai J, Powell DW, Yu D, Kuehn MH, Tezel G. Neurodegenerative and inflammatory pathway components linked to TNF-alpha/TNFR1 signaling in the glaucomatous human retina. Invest Ophthalmol Vis Sci. 2011; 52:8442–8454. [PubMed: 21917936]
11. Bosco A, Romero CO, Breen KT, Chagovetz AA, Steele MR, Ambati BK, Vetter ML. Minocycline upregulates pro-survival genes and downregulates pro-apoptotic genes in experimental glaucoma. Dis Mod Mech. 2015; 8(5):443–455.
12. Nakazawa T, Nakazawa C, Matsubara A, Noda K, Hisatomi T, She H, Michaud N, Hafezi-Moghadam A, Miller JW, Benowitz LI. Tumor necrosis factor-alpha mediates oligodendrocyte death and delayed retinal ganglion cell loss in a mouse model of glaucoma. J Neurosci. 2006; 26(49):12633–12641. [PubMed: 17151265]
13. Roh M, Zhang Y, Murakami Y, Thanos A, Lee SC, Vavvas DG, Benowitz LI, Miller JW. Etanercept, a widely used inhibitor of tumor necrosis factor-α (TNFα), prevents retinal ganglion cell loss in a rat model of glaucoma. PLoS One. 2012; 7(7):e40065. [PubMed: 22802951]
14. Yuan L, Neufeld AH. Activated microglia in the human glaucomatous optic nerve head. J Neurosci Res. 2001; 64(5):523–32. [PubMed: 11391707]
15. Howell GR, Soto I, Zhu X, Ryan M, Macalinao DG, Sousa GL, Caddle LB, MacNicoll KH, Barbay JM, Porciatti V, Anderson MG, Smith RS, Clark AF, Libby RT, John SWM. Radiation treatment inhibits monocyte entry into the optic nerve head and prevents neuronal damage in a mouse model of glaucoma. J Clin Invest. 2012; 122(4):1246–1261. [PubMed: 22426214]
16. Suda T, Takahashi T, Golstein P, Nagata S. Molecular cloning and expression of the Fas ligand, a novel member of the tumor necrosis factor family. Cell. 1993; 75(6):1169–1178. [PubMed: 7505205]
17. Ju ST, Panka DJ, Cui H, Ettinger R, El-Khatib M, Sherr DH, Stanger BZ, Marshak-Rothstein A. Fas (CD95)/FasL interactions required for programmed cell death after T-cell activation. Nature. 1995; 373:444–448. [PubMed: 7530337]
18. Brunner T, Mogli RJ, LaFace D, Yoo NJ, Mahboubi A, Echeverri F, Martin SJ, Force WR, Lynch DH, Ware CF, Green DR. Cell-autonomous Fas (CD95)/Fas-ligand interaction mediates activation-induced apoptosis in T-cell hybridomas. Nature. 1995; 373:441–444. [PubMed: 7530336]
19. Dhein J, Walczak H, Baumler C, Debatin KM, Krammer PH. Autocrine T-cell suicide mediated by APO-1/(Fas/CD95). Nature. 1995; 373(6513):438–441. [PubMed: 7530335]
20. Wajant H, Pfizenmaier K, Scheurich P. Non-apoptotic Fas signaling. Cytokine and Growth Factor Rev. 2003; 14:53–66. [PubMed: 12485619]
21. Lambert C, Landau AM, Desbarats J. Fas-beyond death: A regenerative role for Fas in the nervous system. Apoptosis. 2003; 8:551–562. [PubMed: 14574061]
22. Saas P, Boucraut J, Quiquerez AL, Schnuriger V, Perrin G, Desplat-Jego S, Bernard D, Walker PR, Dietrich PY. CD95 (Fas/Apo-1) as a receptor governing astrocyte apoptotic or inflammatory responses: A key role in brain inflammation. J Immunol. 1999; 162:2326–2333. [PubMed: 9973511]
23. Choi C, Benveniste EN. Fas ligand/Fas system in the brain: regulator of immune and apoptotic responses. Brain Res Rev. 2004; 44(1):65–81. [PubMed: 14739003]
24. Tanaka M, Itai T, Adachi M, Nagata S. Downregulation of Fas ligand by shedding. Nat Med. 1998; 4(1):31–36. [PubMed: 9427603]
25. Hohlbaum AH, Moe S, Marshak-Rothstein A. Opposing effects of transmembrane and soluble Fas ligand expression on inflammation and tumor cell survival. J Exp Med. 2000; 191:1209–1219. [PubMed: 10748238]
26. Suda T, Hashimoto H, Tanaka M, Ochi T, Nagata S. Membrane Fas ligand kills human peripheral blood T lymphocytes, and soluble Fas ligand blocks the killing. J Exp Med. 1997; 186:2045–2050. [PubMed: 9396774]
27. Gregory MS, Marshak-Rothstein A, Hackett CG, Abernathy EF, Moody KS, Hobson M, Lee K, Chen DF, Ksander BR. The form of Fas Ligand determines retinal ganglion cell survival during glaucoma. PLOS ONE. 2011; 6(3):e17659. [PubMed: 21479271]

Author Manuscript Author Manuscript Author Manuscript Author Manuscript

28. Hohlbaum AM, Gregory MS, Ju ST, Marshak-Rothstein A. Fas ligand engagement of resident peritoneal macrophages in vivo induces apoptosis and the production of neutrophil chemotactic factors. J Immunol. 2001; 167:6217–6224. [PubMed: 11714783]
29. Griffith TS, Brunner T, Fletcher SM, Green DR, Ferguson TA. Fas ligand-induced apoptosis as a mechanism of immune privilege. Science. 1995; 270:1189–1192. [PubMed: 7502042]
30. Ju KR, Kim HS, Kim JH, Lee NY, Park CK. Retinal glial cell responses and Fas/FasL activation in rats with chronic ocular hypertension. Brain Res. 2006; 1122:209–221. [PubMed: 17045251]
31. Gregory MS, Repp A, Hohlbaum AM, Marshak-Rothstein A, Ksander BR. Membrane Fas ligand activates innate immunity and terminates ocular immune privilege. J Immunol. 2002; 169:2727–2735. [PubMed: 12193747]
32. Gregory MS, Saff RR, Marshak-Rothstein A, Ksander BR. Control of ocular tumor growth and metastatic spread by soluble and membrane Fas ligand. Cancer Res. 2007; 67:11951–11958. [PubMed: 18089826]
33. Chen H, Wei X, Cho KS, Chen GM, Sappington R, Calkins DJ, Chen DF. Optic neuropathy due to microbead-induced elevated intraocular pressure in the mouse. Invest Ophthalmol Vis Sci. 2011; 52:36–44. [PubMed: 20702815]
34. Dordea AC, Bray MA, Allen K, Logan DJ, Fei F, Malhotra R, Gregory MS, Carpenter AE, Buys ES. An open-source computational tool to automatically quantify immunolabeled retinal ganglion cells. Exp Eye Res. 2016; 147:50–6. [PubMed: 27119563]
35. Karray S, Kress C, Cuvellier S, Hue-Beauvais C, Damotte D, Babinet C, Levi-Strauss M. Complete loss of Fas ligand gene causes massive lymphoproliferation and early death, indicating a residual activity of gld allele. J Immunol. 2004; 172(4):2118–25. [PubMed: 14764677]
36. John SWM, Smith RS, Savinova OV, Hawes NL, Chang B, Turnbull D, Davisson M, Roderick TH, Heckenlively JR. Essential iris atrophy, pigment dispersion, and glaucoma in DBA/2J mice. Invest Ophthalmol Vis Sci. 1998; 39:951–962. [PubMed: 9579474]
37. Libby RT, Li Y, Savinova OV, Barter J, Smith RS, Nickells RW, John SWM. Susceptibility to neurodegeneration in glaucoma is modified by Bax gene dosage. Plos Genetics. 2005; 1:17–26. [PubMed: 16103918]
38. Howell GR, Libby RT, Marchant JK, Wilson LA, Cosma IM, Smith RS, Anderson MG, John SW. Absence of glaucoma in DBA/2J mice homozygous for wild-type versions of Gpnmb and Tyrp1. BMC Genet. 2007; 8:45. [PubMed: 17608931]
39. Howell GR, Libby RT, Jakobs TC, Smith RS, Phalan FC, Barter JW, Barbay JM, Marchant JK, Mahesh N, Porciatti V, Whitmore AV, Masland RH, John SW. Axons of retinal ganglion cells are insulted in the optic nerve early in DBA/2J glaucoma. J cell Biol. 2007; 179:1523–1537. [PubMed: 18158332]
40. Quigley HA, Nickells RW, Kerrigan LA, Pease ME, Thibault DJ, Zack DJ. Retinal ganglion cell death in experimental glaucoma and after axotomy occurs by apoptosis. Invest Ophthalmol Vis Sci. 1995; 36(5):774–786. [PubMed: 7706025]
41. Kerrigan LA, Zack DJ, Quigley HA, Smith SD, Pease ME. TUNEL-positive ganglion cells in human primary open-angle glaucoma. Arch Ophthamol. 1997; 115(8):1031–1035.
42. Levkovitch-Verbin H, Dardik R, Vander S, Nisgav Y, Kalev-Landoy M, Melamed S. Experimental glaucoma and optic nerve transection induce simultaneous upregulation of proapoptotic and prosurvival genes. Invest Ophthalmol Vis Sci. 2006; 47(6):2491–2497. [PubMed: 16723461]
43. Martinez-Lorenzo MJ, Alava MA, Gamen S, Kim KJ, Chuntherapai A, et al. Involvement of APO2 ligand/TRAIL in activation-induced death of Jurkat and human peripheral blood T cells. Eur J Immunol. 1998; 28:2714–2725. [PubMed: 9754559]
44. Powell WC, Fingelton B, Wilson CL, Boothby M, Matrisian LM. The metalloproteinase matrilysin proteolytically generates active soluble Fas ligand and potentiates epithelial cell apoptosis. Curr Biol. 1999; 9:1441–1447. [PubMed: 10607586]
45. Bringmann A, Pannicke T, Grosche J, Francke M, Wiedemann P, Skatchkov SN, Osborne NN, Reichenbach A. Muller cells in the healthy and diseased retina. Prog Retin Eye Res. 2006; 25:397–424. [PubMed: 16839797]

Author Manuscript Author Manuscript Author Manuscript Author Manuscript

46. Wang X, Tay SS, Ng YK. An immunohistochemical study of neuronal and glial cell reactions in retinae of rats with experimental glaucoma. Exp Brain Res. 2000; 132:476–484. [PubMed: 10912828]
47. Tanihara H, Hangai M, Sawaguchi S, Abe H, Kageyama M, Nakazawa F, Shirasawa E, Honda Y. Up-regulation of glial fibrillary acidic protein in the retina of primate eyes with experimental glaucoma. Arch Ophthalmol. 1997; 115:752–756. [PubMed: 9194727]
48. Falvo JV, Tsytsykova AV, Goldfeld AE. Transcriptional control for the TNF gene. Curr Dir Autoimmun. 2010; 11:27–60. [PubMed: 20173386]
49. Zhu W, Downey JS, Gu J, Padova F, Gram H, Han J. Regulation of TNF expression by multiple mitogen-activated protein kinase pathways. J Immunol. 2000; 64(12):6349–6358.
50. Izquierdo E V, Cuevas D, Fernandez-Arroyo S, Riera-Borrull M, Orta-Zavalza E, Joven J, Rial E, Corbi AL, Escribese MM. Reshaping of human macrophage polarization through modulation of glucose catabolic pathways. J Immuunol. 2015; 195:2442–2451.
51. Tonari M, Kurimoto T, Horie T, Sugiym T, Ikeda T, Oku H. Blocking endothelin-B receptors rescues rential ganglion cells from optic nerve injury through suppression of neuroinflammation. Invest Ophthalmol Vis Sci. 2012; 53:3490–3500. [PubMed: 22562513]
52. Ahmad S, Fatteh N, El-Sherbiny N, Naime M, Ibrahim AS, El-Sherbini AM, El-Shafey SA, Khan S, Fulzele S, Gonzales J, Liou GI. Potential role of A_{2A} adenosine receptor in traumatic optic neuropathy. J Neruoimmunol. 2013; 264:54–64.
53. Zhou X, Li F, Kong L, Chodosh J, Cao W. Anti-inflammatory effect of pigment epithelium-derived factor in DBA.2J mice. Mol Vis. 2009; 15:438–450. [PubMed: 19247457]
54. Howell GR, Macalinao DG, Sousa GL, Walden M, Soto I, Kneeland SC, Barbay JM, King BL, Marchany JK, Hibbs M, Stevens B, Barres BA, Clark AF, Libby RT, John SWM. Molecular clustering identifies complement and endothelin induction as early events in a mouse model of glaucoma. J Clin Invest. 2011; 121:1429–1444. [PubMed: 21383504]
55. Yuan L, Neufeld AH. Tumor necrosis factor-alpha: a potentially neurodestructive cytokine produced by glia in the human glaucomatous optic nerve head. Glia. 2000; 32:42–50. [PubMed: 10975909]
56. Tezel G, Li LY, Patil RV, Wax MB. TNF-alpha and TNF-alpha receptor-1 in the retina of normal and glaucomatous eyes. Invest Ophthalmol Vis Sci. 2001; 42:1787–1794. [PubMed: 11431443]
57. Zho Y, Pernet V, Hauswirth WW, Di Polo A. Activation of the extracellular signal-regulated kinase 1/2 pathway by AAV gene transfer protects retinal ganglion cells in glaucoma. Mol Ther. 2005; 12:402–412. [PubMed: 15975850]
58. Pease ME, Zack DJ, Berlinicke C, Bloom K, Cone F, Wang Y, Klein RL, Hauswirth WW, Quigley HA. Effect of CNTF on retinal ganglion cell survival in experimental glaucoma. Invest Ophthalmol Vis Sci. 2009; 50:2194–200. [PubMed: 19060281]
59. Ju WK, Kim KY, Duong-Polk KX, Lindsey JD, Ellisman MH, Weinreb RN. Increased optic atrophy type 1 expression protects retinal ganglion cells in a mouse model of glaucoma. Mol Vis. 2010; 16:1331–1342. [PubMed: 20664796]
60. Almasieh M, Wilson AM, Morquette B, Vargas JLC, Di Polo A. The molecular basis of retinal ganglion cell death in glaucoma. Prog Ret Eye Res. 2012; 31:152–181.
61. Libby RT, Li Y, Savinova OV, Barter J, Smith RS, Nickelles RW, John SW. Susceptibility to neurodegeneration in glaucoma is modified by Bax gene dosage. PLoS Genet. 2005; 1(1):17–26. [PubMed: 16103918]
62. Zhou X, Li F, Kong L, Tomita H, Li C, Cao W. Involvement of inflammation, degradation, and apoptosis in a mouse model of glaucoma. J Biol Chem. 2005; 280(35):31240–31248. [PubMed: 15985430]
63. Yang Z, Quigley HA, Pease ME, Yang Y, Qian J, Valenta D, Zack DJ. Changes in Gene Expression in Experimental Glaucoma and Optic Nerve Transection: The Equilibrium between Protective and Detrimental Mechanisms. Invest Ophthalmol Vis Sci. 2007; 48:5539–5548. [PubMed: 18055803]
64. Ferguson TA, Apte RS. Angiogenesis in eye disease: immunity gained or immunity lost? Semin Immunopathol. 2008; 30:111–119. [PubMed: 18297288]

Author Manuscript Author Manuscript Author Manuscript Author Manuscript

65. Vernet-der Garabedian B, Dere P, Bailly Y, Mariani J. Innate immunity in the Grid2Lc/+ mouse model of cerebeller neurodegeneration: glial CD95/CD95L plays a non-apoptotic role in persistent neuron loss-associated inflammatory reactions in the cerebellum. J Neuroinflamm. 2013; 10:65.

66. Sabelko KA, Kelly KA, Nahm MH, Cross AH, Russell JH. Fas and Fas ligand enhance the pathogenesis of experimental allergic encephalomyelitis, but are not essential for immune privilege in the central nervous system. J Immunol. 1997; 159:3096–3099. [PubMed: 9317103]

67. Matsumoto H, murakami Y, Kataoka K, Notomi S, Mantopoulos D, Trochons G, Miller JW, Gregory MS, Ksander BR, Marshak-Rothstein A, Vavvas DG. Membrane-bound and soluble Fas ligands have opposite functions in photoreceptor cell death following separation from the retinal pigment epithelium. Cell Death Dis. 2015; 6:e1986. [PubMed: 26583327]

68. Bossaller L, Chiang PI, Schmidt-Lauber C, Ganesan S, Kaiser WJ, Rathinam VAJ, Mocarski ES, Subramanian D, Green DR, Silverman N, Fitzgerald KA, Marsha-Rothstein A, Latz E. Cutting Edge: FAS (CD95) mediates noncanonical IL-1b and IL-18 maturation via casapse-8 in an RIP3-independent manner. J Immunol. 2012; 189:5508–5512. [PubMed: 23144495]

69. Kim IB, Kim KY, Joo CK, Lee MY, Oh SJ, Chung JW, Chun MH. Reaction of Muller cells after increased intraocular pressure in the rat retina. Exp Brain Res. 1998; 121:419–424. [PubMed: 9746148]

70. Yang X, Hondur G, Tezel G. Antioxidant treatment limits neuroinflammation in experimental glaucoma. Invest Ophthalmol Vis Sci. 2016; 57(4):2344–2354. [PubMed: 27127934]

71. Batchelor JR, Casey TA, Gibbs DC. HLA matching and corneal grafting. Lancet. 1976; 1:551–554. [PubMed: 55836]

72. Price FW, Whitson WE, Marks RG. Progression of visual acuity after penetrating keratoplasty. Ophthalmology. 1991; 98:1177–1185. [PubMed: 1923353]

73. Sano Y, Ksander BR, Streilein JW. Fate of orthotopic corneal allografts in eyes that cannot support anterior chamber-associated immune deviation induction. Invest Ophthalmol Vis Sci. 1995; 36(11):2176–2185. [PubMed: 7558710]

74. Stuart PM, Griffith TS, Usui N, Pepose J, Yu X, Ferguson TA. CD95 ligand (FasL)-induced apoptosis is necessary for corneal graft survival. J Clin Invest. 1997; 99(3):396–402. [PubMed: 9022072]

75. Sano Y, Yamada J, Ishino Y, Adachi W, Kawasaki S, Suzuki T, Kinoshita S, Okuyama T, Azuma N. Non-cleavable mutant Fas ligand transfection of donor cornea abrogates ocular immune privilege. Exp Eye Res. 2002; 75:475–483. [PubMed: 12387794]

76. Stankowska DL, Minton AZ, Rutledge MA, Muelle BH, Phatak NR, He S, Ma HY, Forster MJ, Yorio T, Krishnamoorthy RR. Neuroprotective effects of transcription factor Brn3b in an ocular hypertension rat model of glaucoma. Invest Ophthalmol Vis Sci. 2015; 56(2):893–907. [PubMed: 25587060]

77. McKinnon SJ, Lehman DM, Tahzib NG, Ransom NL, Reitsamer HA, Liston P, LaCase E, Li Q, Korneluk RG, Hauswirth WM. Baculoviral IAP repeat-containing-4 protects optic nerve axons in a rat glaucoma model. Mol Therapy. 2002; 5(6):780–787.

78. Tezel G, Yang X, Cai J. Proteomic identification of oxidatively modified retinal proteins in a chronic pressure-induced rat model of glaucoma. Invest Ophthalmol Vis Sci. 2005; 46:3177–3187. [PubMed: 16123417]

79. Pache M, Flammer J. A sick eye in a sick body? Systemic findings in patients with primary open-angle glaucoma. Survey Ophthalmol. 2006; 51(3):179–212.

80. Nucci C, Tartaglione R, Rombola L, Morrone LA, Fazzi E, Bagetta G. Neurochemical evidence to implicate elevated glutamate in the mechanisms of high IOP-induced retinal ganglion cell death in rat. Neurotox. 2005; 26(5):935–941.

81. Ali RR, Reichel MB, De Alwis M, Kanuga N, Kinnon C, Levinsky RJ, Hunt DM, Bhattachatya SS, Thrasher AJ. Adeno-associated virus gene transfer to mouse retina. Human Gen Ther. 1998; 9(1): 81–86.

82. Dudus L, Anand V, Acland GM, Chen SJ, Wilson JM, Fisher KJ, Maguire AM, Bennet J. Persistent transgene product in the retina, optic nerve, and brain after intraocular injection of rAAV. Vis Res. 1999; 39(150):2545–53. [PubMed: 10396623]

Author Manuscript Author Manuscript Author Manuscript Author Manuscript

83. Sullivan TA, Geisert EE, Hines-Beard J, Rex TS. Systemic adeno-associated virus-mediated gene therapy preserves reitnal ganglion cells and visual function in DBA/2J glaucomatous mice. Human Gen Ther. 2001; 22:1191–1200.

84. Bond WS, Hines-Beard J, Golden Merry YL, Davis M, Farooque A, Sappington RM, Calkins DJ, Rex TS. Virus-mediated EpoR76E therapy slows optic nerve axonopathy in experimental glaucoma. Mol Ther. 2016; 24(2):230–239. [PubMed: 26502777]

Author Manuscript Author Manuscript Author Manuscript Author Manuscript

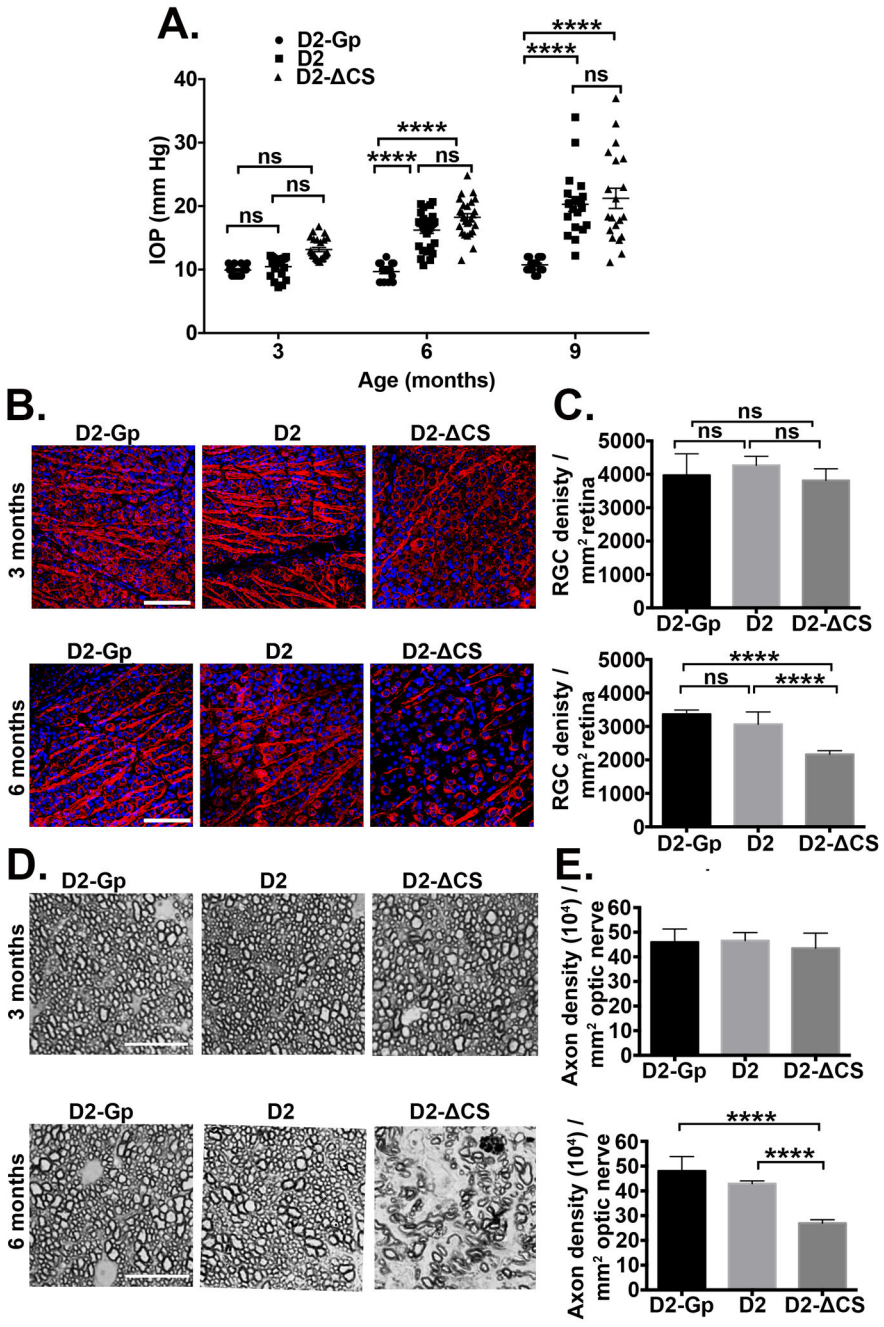

Fig 1. Accelerated loss of RGCs and axons in D2-ΔCS mice

(A) IOP measurements were taken by rebound tonometry in D2-Gp, D2, and D2-ΔCS mice at 3, 6, and 9 months of age (N=16 D2-GP; N=22 D2, N=22 D2-ΔCS). Data is presented as mean IOP ± SEM. (B) Representative confocal images of retinal flat-mounts isolated from D2-Gp, D2, and D2-ΔCS mice at 3 and 6 months of age, stained with β-III tubulin (red) a RGC-specific marker and DAPI a nuclear stain (blue) (Scale bar, 75μm). (C) Quantification of β-III tubulin positive RGCs, represented as RGC density/mm^2 retina. N=10 eyes per group. (D) Representative photomicrographs of PPD optic nerve cross sections taken from

Author Manuscript Author Manuscript Author Manuscript Author Manuscript

D2-Gp, D2 and D2-ΔCS at 3 and 6 months of age (Scale bar, 10μm). (E) Quantification of healthy axons, represented as axon density $(10^4)/mm^2$ ON. N=10 optic nerves per group. Ns, non-significant, ****P<0.0001.

Author Manuscript Author Manuscript Author Manuscript Author Manuscript

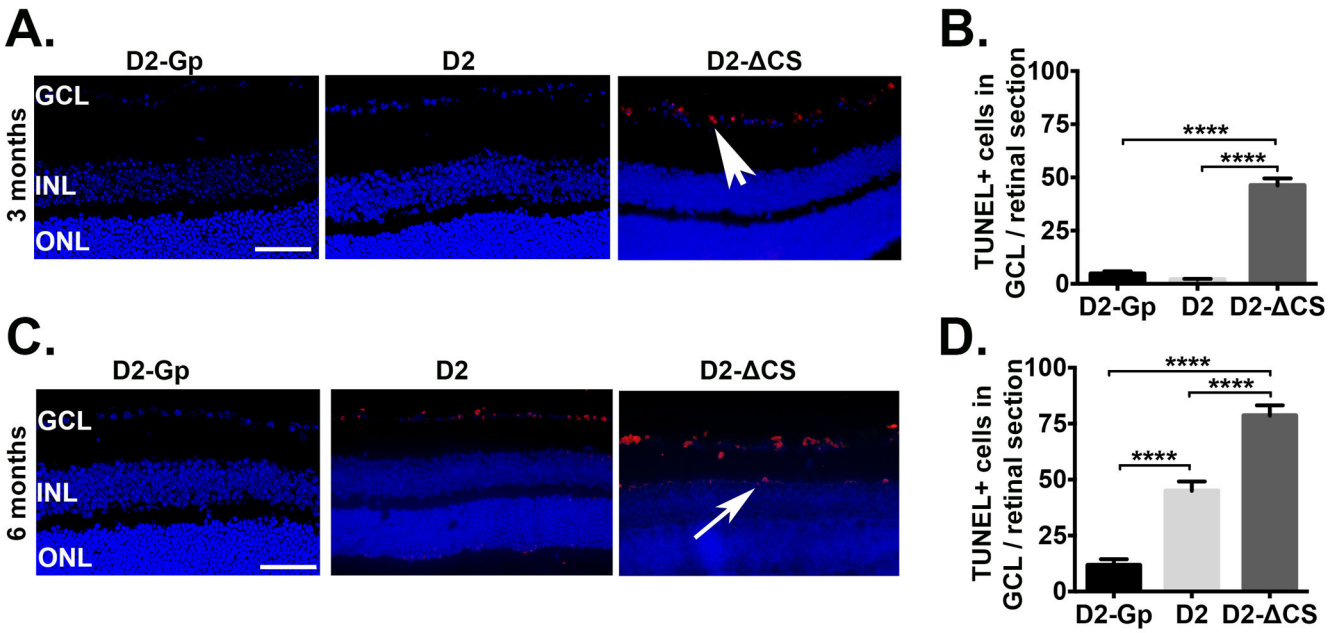

Fig 2. Accelerated apoptosis coincides with RGC loss in the absence of sFasL

Representative TUNEL staining in paraffin embedded retinal sections taken from D2-Gp, D2 and D2-ΔCS mice at (A) 3 and (C) 6 months of age (Scale bar, 100μm). TUNEL = red, DAPI, nuclear marker = blue. GCL, ganglion cells layer; INL, inner nuclear layer; ONL, outer nuclear layer. White arrowhead = TUNEL positive cells in GCL, white arrow = TUNEL positive cells in INL. TUNEL positive cells in the GCL were quantitated at (B) 3 months and (D) 6 months of age, shown as the number of TUNEL positive cells in the GCL/ retinal section (9 sections/retina), N=8 per group. ****P<0.0001.

Author Manuscript Author Manuscript Author Manuscript Author Manuscript

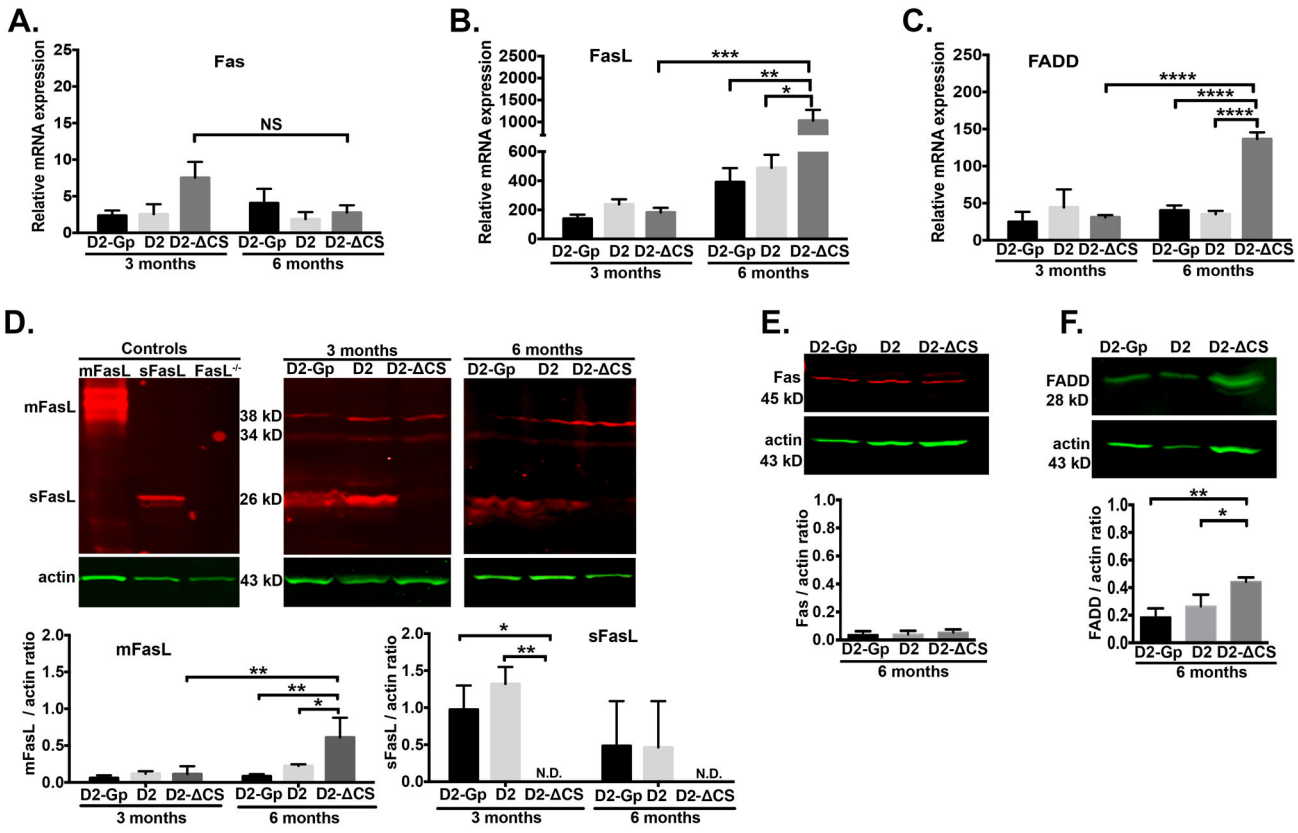

Fig 3. Expression of Fas, FasL, and FADD in D2-ΔCS mice

Quantitative RT-PCR was performed on the neural retina isolated from D2-GP, D2, and D2-ΔCS mice at 3 and 6 months of age to quantitate mRNA levels of: (A) Fas, (B) FasL, and (C) FADD. N=6 per group. Representative Western blots from protein lysates (20μg/sample) prepared from posterior eye cups isolated from D2-GP, D2, and D2-ΔCS mice for (D) FasL at 3 and 6 months (actin is green, FasL is red), (E) Fas at 6 months (actin is green, Fas is red), and (F) FADD at 6 months (actin is green, FADD is green). Protein lysates prepared from L5178Y-R tumor cells transfected with sFasL or mFasL vectors (31) were used as positive controls for FasL and the protein lysate from posterior eyecups of FasL-KO mice (27, 35) was used as a negative control for FasL. Densitometry analysis of mFasL (34 and 38 kD bands), sFasL (26 kD band), Fas (43 kD), and FADD (28 kD) is the average of 3 independent experiments (3 independent blots consisting of 1 posterior segment per group, per experiment) Error bars indicate SEM; N.D.- not detected (below the level of detection by densitometry). *P<0.05, **P<0.01, ****P<0.0001.

Author Manuscript Author Manuscript Author Manuscript Author Manuscript

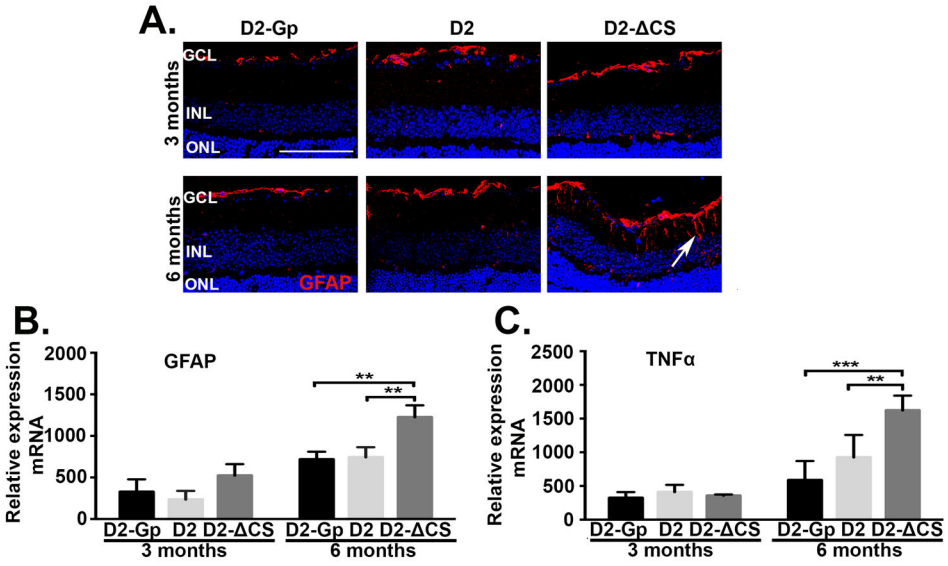

Fig 4. Expression of GFAP and TNFα in the retina of D2-ΔCS mice

(A) Representative confocal microscopy images of paraffin embedded retinal sections taken from D2-Gp, D2, and D2-ΔCS mice at (A) 3 and 6 months of age and stained for GFAP (red) and DAPI (blue). (white arrow=GFAP in muller cells, Scale bar, 100μm). Quantitative RT- PCR was performed on the neural retina isolated from D2-GP, D2, and D2-ΔCS mice at 3 and 6 months of age to quantitate mRNA levels of (B) GFAP and (C) TNFα. N=6 per group. Error bar indicates SEM. **<0.01 and ***P<0.001.

Author Manuscript Author Manuscript Author Manuscript Author Manuscript

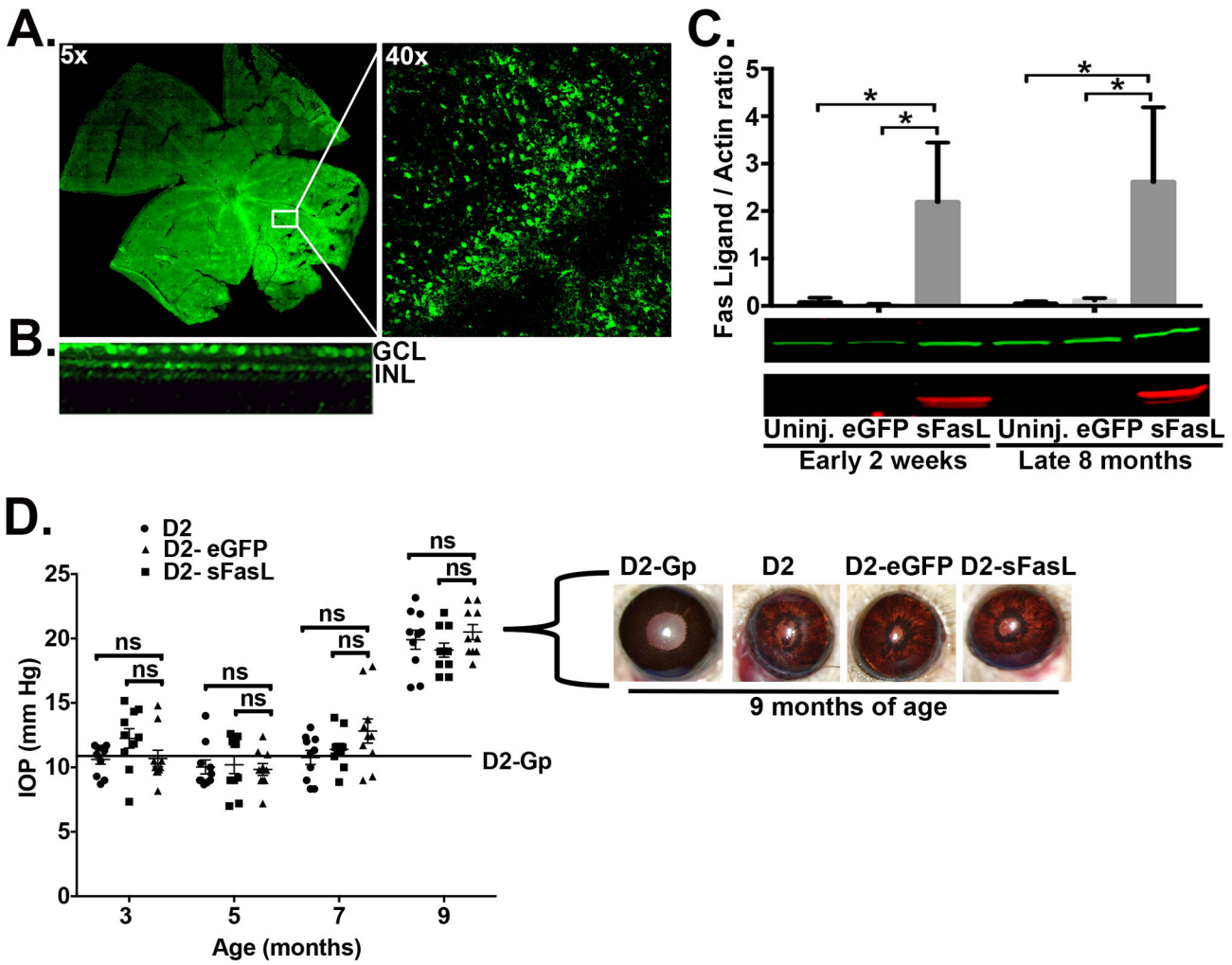

Fig 5. Over expression of sFasL in D2 mice

D2 mice received one intravitreal injection of AAV2.sFasL or AAV2.eGFP as a control at 2 months of age. (A) Retinal flat-mount showing expression of AAV2.eGFP throughout the retina (Magnification, 5x and 40x). (B) Cross sectional 3-D reconstruction of the retina. GCL-ganglion cell layer, INL-inner nuclear layer. (C) Western blot from neural retinal lysates (5μg/sample, sFasL is red band, actin is green band) showing overexpression of sFasL (26 kD) at both 2wk and at 8 months post AAV2 injection. N=3 per group. Densitometry is the average of 3 independent experiments (3 independent blots consisting of 1 neural retina per group, per experiment). (D) IOP measurements were taken at 3, 5, 7, and 9 months of age by rebound tonometry in D2 (uninjected), D2-AAV2.eGFP, and D2-AAV2.sFasL. Mean IOP for the D2-Gp non-glaucomatous control group is 12 mmHg ±3 SEM, identified as an solid line on the IOP graph. Data is presented as mean IOP ± SEM IOP (N=10 per group). Representative slit lamp images taken at 9 months of age show pigment dispersion and iris stromal atrophy in D2-Gp, D2 (uninjected), D2-AAV.eGFP, and D2-AAV.sFasl mice. Ns, non-significant, *P<0.05.

Author Manuscript Author Manuscript Author Manuscript Author Manuscript

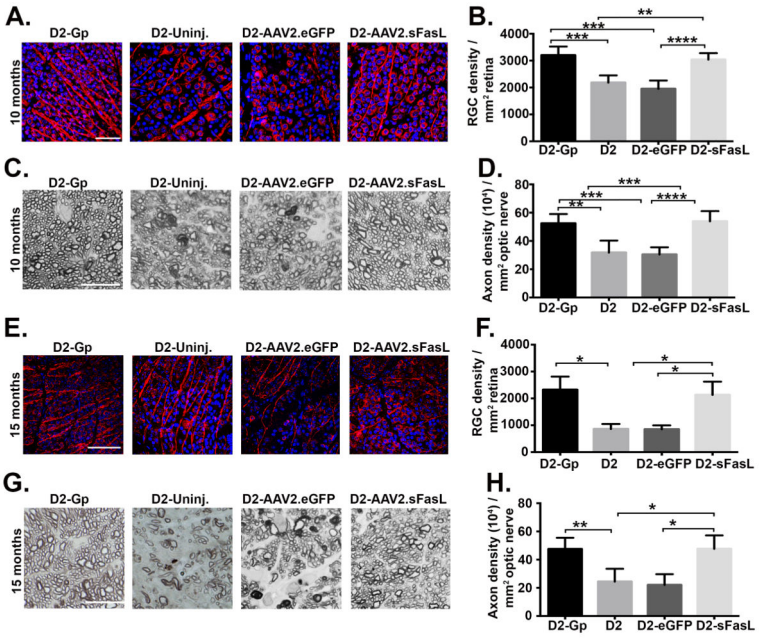

Fig 6. Intravitreal AAV2.sFasL protects RGCs and axons in D2 mice

D2 mice received one intravitreal injection of AAV2.sFasL or AAV2.eGFP as a control at 2 months of age. At 10 and 15 months of age, AAV2.sFasL and AAV2.eGFP treated mice, in addition to age-matched D2-uninj (uninjected) and D2-Gp mice were euthanized and retinas and optic nerves processed for analysis of RGC and axon density. (A) Representative confocal images of retinal flat-mounts isolated from 10 month old D2-Gp, D2 uninjected, D2-AAV2.eGFP and D2-AAV2.sFasL mice, stained with β-III tubulin (red) an RGC-specific marker and DAPI a nuclear stain (blue). (Scale bar, 50μm). (B) Quantification of β-III tubulin positive RGCs, represented as RGC density/mm^2 retina. N=10 per group (C) Representative photomicrographs of PPD stained optic nerve cross sections taken from 10 month old D2-Gp, D2 uninjected, D2-AAV2.eGFP and D2-AAV2.sFasL mice (Scale bar, 10μm). (D) Quantification of healthy axons, represented as axon density (10^4)/mm^2. N=10 per group (E) Representative confocal images of retinal flat-mounts isolated from 15 month old D2-Gp, D2 uninjected, D2-AAV2.eGFP and D2-AAV2.sFasL mice, stained with β-III tubulin (red) an RGC-specific marker and DAPI a nuclear stain (blue) (Scale bar, 75μm). (F) Quantification of β-III tubulin positive RGCs, represented as RGC density/mm^2 retina. N=5 per group. (G) Representative photomicrographs of PPD optic nerve cross sections taken from 15 month old D2-Gp, D2 uninjected, D2-AAV2.eGFP and D2-AAV2.sFasL mice (Scale bar, 10μm). (H) Quantification of healthy axons, represented as axon density (10^4)/mm^2. N=5 per group. *P<0.05, **P<0.01, ***P<0.001 ****P<0.0001

Author Manuscript Author Manuscript Author Manuscript Author Manuscript

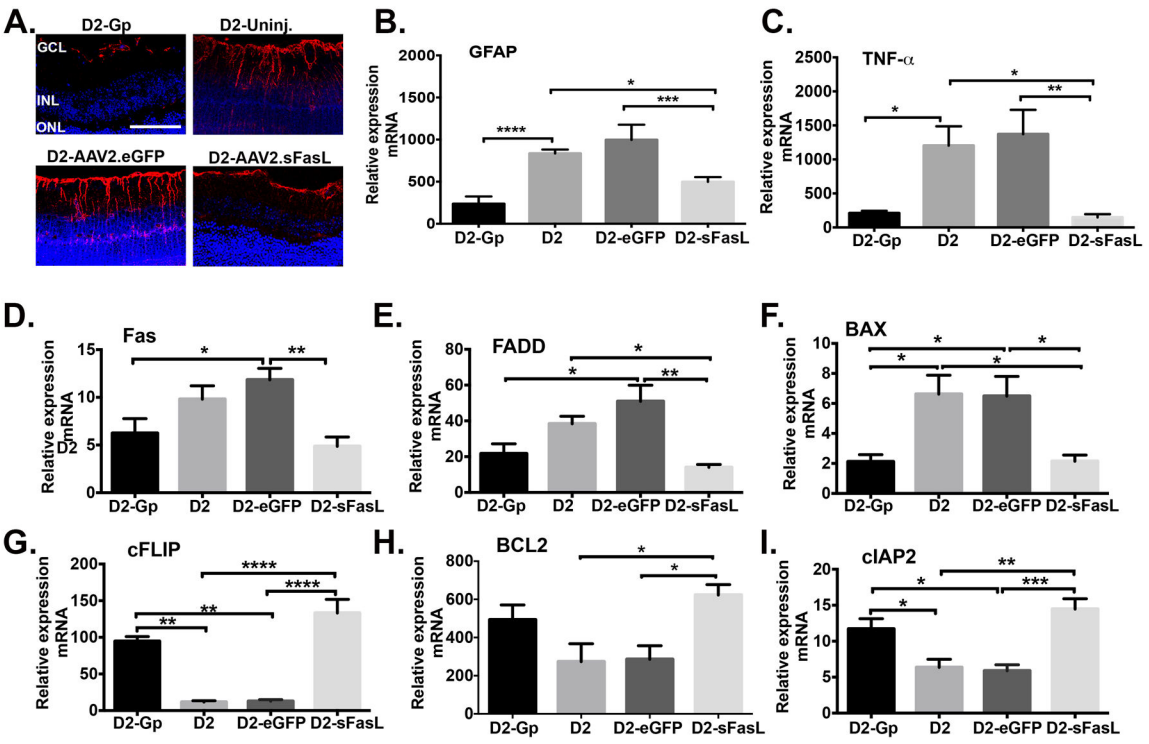

Fig 7. Muller glial cell activation and induction of inflammatory and apoptotic mediators in the retina of D2 mice treated with AAV2.sFasL

(A) Representative confocal microscopy images of paraffin embedded retinal sections taken from D2-Gp, D2-uninj. D2-AAV2-eGFP, and D2-AAV2-sFasL mice at 10 months of age and stained for GFAP (red) and DAPI (blue) (Scale bar, 100μm). Quantitative RT- PCR was performed on the neural retina isolated from D2-Gp, D2-uninj., D2-AAV2-eGFP, and D2-AAV2-sFasL mice at 10 months of age to quantitate mRNA levels of (B) GFAP, (C) TNFα, (D) pro-apoptotic mediators Fas, FADD, and BAX, and (E) anti-apoptotic mediators cFLIP, Bcl2, and cIAP2. N=5–6 per group. Error bar indicates SEM. *P<0.05, **<0.01, ***P<0.001, ****<0.0001.

Author Manuscript Author Manuscript Author Manuscript Author Manuscript

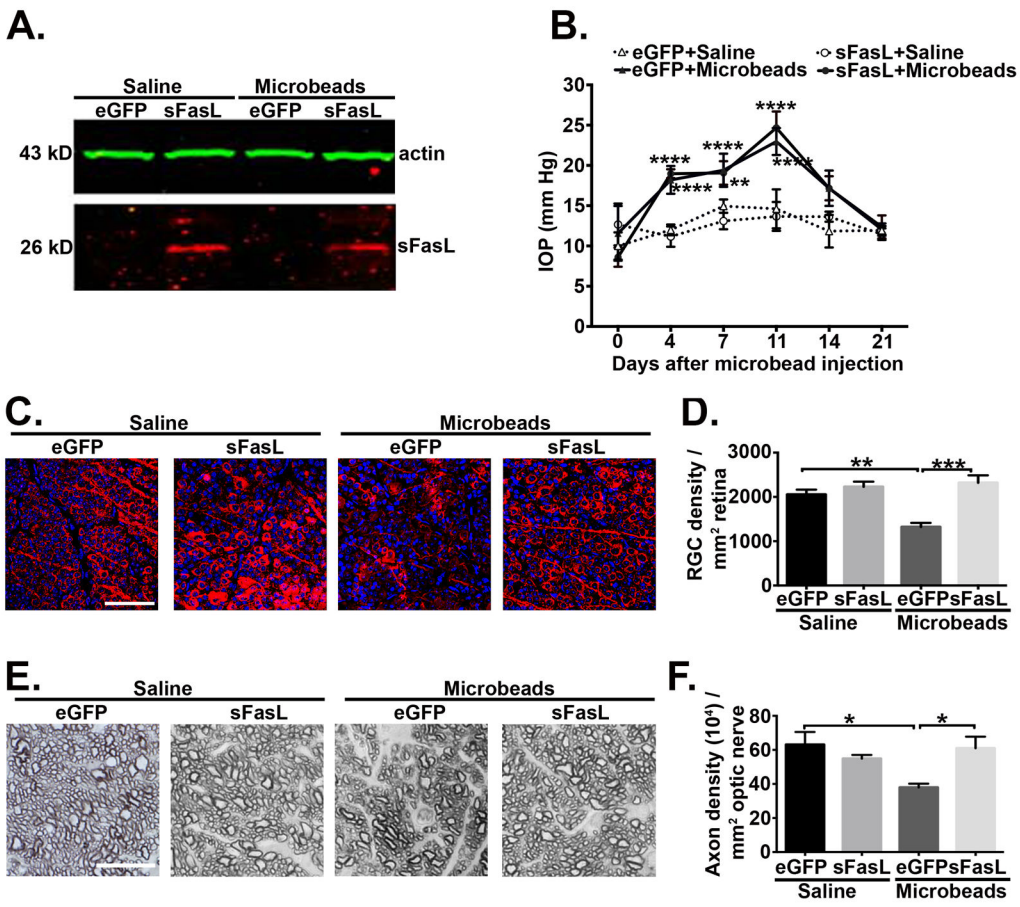

Fig. 8. Pre treatment with AAV2.sFasL protects RGC cell death in microbead-induced mouse model of elevated IOP in C57/BL6 mice

(A) Western blot from neural retina lysates (5ug/sample) showing overexpression of sFasL at 26 kD (Red band) and actin (Green band) in saline and microbead injected B6.AAV2.eGFP and B6.AAV2.sFasL mice at 4 weeks post microbead or saline injections. (B) IOP measurements were taken by rebound tonometry from B6.AAV2.eGFP and B6.AAV2.sFasL mice treated with saline or microbeads. Data is presented as mean IOP ± SEM, (N=10 per group). At 28 days post microbead injection the neural retina and optic nerve were processed for quantification of RGC and axon density. (C) Representative confocal microscopic images from retinal flat-mounts stained with βIII tubulin (red), an RGC-specific marker and DAPI a nuclear stain (blue) at 4 weeks post microbead or saline injections (Scale bar, 75μm). (D) Quantification of β-III tubulin positive RGCs, represented as RGC density/mm^2 retina (E) Representative photomicrographs of optic nerve cross sections stained with PPD at 4 weeks post microbead or saline injections (Scale bar, 10μm). (F) Quantification of healthy axons, represented as axon density (10^4)/mm^2. N=5 per group. *P<0.05, **P<0.01, ***P<0.001, ****P<0.0001.

Author Manuscript Author Manuscript Author Manuscript Author Manuscript

Table I

List of RNA primers used for Real time PCR

		Primers	Sequence
1)	Forward	TNF-α	5′-GGG ACA GTG ACC TGG ACT GT-3′
2)	Reverse	TNF-α	5′-CTC CCT TTG CAG AAC TCA GG-3′
3)	Forward	β-actin	5′-TGT TAC CAA CTG GGA CGA CA-3′
4)	Reverse	β-actin	5′-CTT TTC ACG GTT GGC CTT AG-3′
5)	Forward	C-FLIP	5′-TTC TGA TAT AGG GTC CTG C-3′
6)	Reverse	C-FLIP	5′-TCA CCA GAT CCA AGA AAC TC-3′
7)	Forward	FADD	5′-CAA GCT GAG TGT AAC TGA AG-3′
8)	Reverse	FADD	5′-TTA AAA GGC ATC AGC AAG AG-3′
9)	Forward	GFAP	5′-GGC GCT CAA TGC TGG CTT CA-3′
10)	Reverse	GFAP	5′-TCT GCC TCC AGC CTC AGG TT-3′
11)	Forward	BAX	5′-AGG GTT TCA TCC AGG ATC GAG CAG-3′
12)	Reverse	BAX	5′-ATC TTC TTC CAG ATG GTG AGC GAG-3′
13)	Forward	BCL-2	5′TTG TGG CCT TCT TTG AGT TCG GTG-3′
14)	Reverse	BCL-2	5′ GGT GCC GGT TCA GGT ACT CAG TCA-3′
15)	Forward	TRADD	GAA GTT CCC GGT TTC CTC TC
16)	Reverse	TRADD	GAG GGC AGG ATC TCT CAG TG
17)	Forward	c-IAP-2	TGT CAG CCA AGT TCA AGC TG
18)	Reverse	c-IAP-2	ATC TTC CGA ACT TTC TCC AGG G
19)	Forward	Fas-L	TGG GTA GAC AGC AGT GCC AC
20)	Reverse	Fas-L	GCC CAC AAG ATG GAC AGG G
21)	Forward	Fas-R	GTC CTG CCT CTG GTG CTT GCT G
22)	Reverse	Fas-R	CAG GTT GGC ATG GTT GA